

CLINICAL STUDY



CircRNA itchy E3 ubiquitin protein ligase improves mitochondrial dysfunction in sepsis-induced acute kidney injury by targeting microRNA-214-3p/ATP-binding cassette A1 axis

Weidi Ye^a, Qi Miao^b, Guangxin Xu^a, Kai Jin^b, Xue Li^a, Weidong Wu^a, Lina Yu^a and Min Yan^a

^aDepartment of Anesthesiology, The Second Affiliated Hospital of Zhejiang University School of Medicine, Hangzhou, P.R. China;

^bZhejiang Provincial Engineering Institute on Eye Diseases, Zhejiang Provincial Key Laboratory of Ophthalmology, Zhejiang Provincial Clinical Research Center for Eye Diseases, Eye Center Second Affiliated Hospital of Zhejiang University School of Medicine, Hangzhou, P.R. China

ABSTRACT

Background: Circular RNAs (circRNAs) are promising biomarkers and therapeutic targets for acute kidney injury (AKI). In this study, we investigated the mechanism by which circRNA itchy E3 ubiquitin protein ligase (circ-ITCH) regulates sepsis-induced AKI.

Methods: A sepsis-induced AKI mouse model was created using LPS induction and circ-ITCH overexpression. Circ-ITCH levels were confirmed *via* RT-qPCR. Kidney tissue changes were examined through various stains and TUNEL. Enzyme-linked immunosorbent assay (ELISA) gauged oxidative stress and inflammation. Mitochondrial features were studied with electron microscopy. RT-qPCR and western blotting assessed mitochondrial function parameters. Using starBase, binding sites between circ-ITCH and miR-214-3p, as well as miR-214-3p and ABCA1, were predicted. Regulatory connections were proven by dual-luciferase assay, RT-qPCR, and western blotting.

Results: Circ-ITCH expression was downregulated in LPS-induced sepsis mice. Overexpression of circ-ITCH ameliorates indicators of renal function (serum creatinine [SCr], blood urea nitrogen [BUN], neutrophil gelatinase-associated lipocalin [NGAL], and kidney injury molecule-1 [Kim-1]), reduces renal cell apoptosis, mitigates oxidative stress markers (reactive oxygen species [ROS] and malondialdehyde [MDA]), and diminishes inflammatory markers (interleukin [IL]-1 β , IL-6, and tumor necrosis factor [TNF- α]). Moreover, circ-ITCH overexpression alleviated mitochondrial damage and dysfunction. Furthermore, circ-ITCH acts as a sponge for miR-214-3p, thereby upregulating ABCA1 expression. In addition, the miR-214-3p inhibitor repressed oxidative stress, inflammation, and mitochondrial dysfunction, which was reversed by circ-ITCH knockdown. Further cellular analysis in HK-2 cells supported these findings, highlighting the protective role of circ-ITCH against sepsis-induced AKI, particularly through the miR-214-3p/ABCA1 axis.

Conclusion: The novel circ-ITCH/miR-214-3p/ABCA1 pathway plays an essential role in the regulation of oxidative stress and mitochondrial dysfunction in sepsis-induced AKI.

ARTICLE HISTORY

Received 9 May 2023
Revised 28 August 2023
Accepted 17 September 2023

KEYWORDS



circ-ITCH;
microRNA-214-3p;
sepsis-induced acute
kidney injury;
mitochondrial
dysfunction; ABCA1


1. Introduction

Sepsis is a severe clinical disorder characterized by disproportionate and harmful responses to infection. This can lead to acute organ dysfunction and a significant risk of mortality [1]. Among individuals with sepsis, the incidence of acute kidney injury (AKI) is estimated at approximately 33%, translating to an annual occurrence rate of around 1 per 1000 people globally [2]. Despite advances in specific therapies, such as resuscitation, vasoactive drugs, and renal replacement, the mortality rate remains high for patients with

sepsis-induced AKI [3]. Therefore, exploring and understanding the molecular mechanisms of sepsis-induced AKI will contribute to the development of novel and effective therapeutic strategies.

Oxidative stress is a critical pathological feature of AKI that results in mitochondrial depolarization and dysfunction [4]. Increased (reactive oxygen species [ROS]) exacerbates mitochondrial damage, which in turn amplifies oxidative stress [5,6]. Mitochondrial damage causes inflammation and promotes the progression of AKI into renal fibrosis [7,8].

CONTACT Min Yan  zryanmin@zju.edu.cn  Department of Anesthesiology, The Second Affiliated Hospital of Zhejiang University School of Medicine, No.88, Jiefang Road, Hangzhou 310000, P.R. China

 Supplemental data for this article can be accessed online at <https://doi.org/10.1080/0886022X.2023.2261552>.

© 2023 The Author(s). Published by Informa UK Limited, trading as Taylor & Francis Group

This is an Open Access article distributed under the terms of the Creative Commons Attribution-NonCommercial License (<http://creativecommons.org/licenses/by-nc/4.0/>), which permits unrestricted non-commercial use, distribution, and reproduction in any medium, provided the original work is properly cited. The terms on which this article has been published allow the posting of the Accepted Manuscript in a repository by the author(s) or with their consent.

Accordingly, alleviation of mitochondrial dysfunction caused by oxidative stress in the kidney is essential for sepsis-induced AKI treatment [9]. Mitochondrial dysfunction in sepsis is also caused by mitochondrial permeability transition (MPT) opening. Oxidative stress can lead to apoptosis by altering MPT [10].

Circular RNAs (circRNAs) are covalently closed endogenous RNAs that participate in cellular development and energy mechanisms [11]. CircRNA *ITCH* E3 ubiquitin-protein ligase (circ-*ITCH*) is a circRNA that is well-known as a tumor suppressor [12]. Su et al. provided a conceptual framework for elucidating the involvement of circ-*ITCH* in cellular functions and inflammatory regulation [13]. Circ-*ITCH* exerts regulatory functions in cells by binding miRNAs [14]. It has been reported that circ-*ITCH* mediates miRNA-mRNA axis in sepsis-stimulated acute lung injury [15]. However, the impact of circ-*ITCH* on sepsis-stimulated AKI remains largely unexplored and requires further exploration. A study reported that circ-*ITCH* targets miR-214 to regulate gene expression [16]. Bioinformatic analysis showed that circ-*ITCH* binds to miR-214-3p. Renal miR-214-3p promotes the development of hypertension [17]. In addition, miR-214-3p aggravates kidney injury and inflammatory responses in hyperlipidemic pancreatitis [18]. Zhou et al. found that miR-214-3p exacerbates tubular epithelial cell ferroptosis in cisplatin-induced AKI [19]. However, it remains unknown whether circ-*ITCH* regulates sepsis-induced AKI by binding miR-214-3p.

The primary objective of this study was to clarify the function and fundamental mechanism of circ-*ITCH* in the development of sepsis-induced AKI. We discovered that circ-*ITCH* improved mitochondrial dysfunction in sepsis-induced AKI by targeting the miR-214-3p/ATP-binding cassette A1 (ABCA1) axis. The circ-*ITCH*/miR-214-3p/ABCA1 axis is a promising target for the treatment of sepsis-induced AKI.

2. Materials and methods

2.1. Mice model

Animal experiments were performed on C57BL/6 mice ($n = 24$) at 8–12 weeks of age procured from GemPharmatech Co. Ltd. Mice were bred and raised for one week under humidity-controlled conditions with free access to food and water. Then, mice were assigned randomly into four groups ($n = 6$ /per group): control, lipopolysaccharide (LPS), oe-NC, and oe-*ITCH* groups. The sepsis-induced AKI mouse model ($n = 18$) for LPS, oe-NC, and oe-*ITCH* groups was constructed by intraperitoneal injection of 16 mg/kg LPS (S1732, Beyotime, China) [20]. Control mice ($n = 6$) were injected with an equal volume of phosphate-buffered saline (PBS; 500 μ L, C0221A, Beyotime, China). After 24 h, serum was collected prior to euthanasia *via* cervical dislocation, after which kidney tissues were harvested. This study was approved by the Institutional Animal Care and Use Committee of the Second Affiliated Hospital of Zhejiang University School of Medicine.

2.2. Cell model

HK-2 cells were procured from the American Type Culture Collection (ATCC). Cells were cultured in the Minimum Essential Medium (MEM, #11090081, Gibco, Carlsbad, CA, USA) with 10% fetal bovine serum at 37°C with 5% CO₂. To create a cellular model of sepsis-induced AKI, HK-2 cells were subjected to 24-h treatment with 1 μ g/mL LPS. We selected 1 μ g/mL LPS based on prior studies [21].

2.3. Transfection

Lentivirus-packaged circ-*ITCH* was used for both overexpression (oe-*ITCH*) and knockdown (sh-*ITCH*) experiments. The respective negative controls, oe-NC and sh-NC, are scrambled sequences unrelated to any known mammalian gene. Additionally, an empty vector, miR-214-3p inhibitor, and an NC inhibitor were sourced from Synthgene (Nanjing, China). For *in vivo* transfection, either oe-*ITCH* or oe-NC was mixed with the Entranster reagent (Engreen, China) and administered intravenously to LPS-induced septic mice. After 24 h, the serum and kidneys were harvested from the mice for further investigation. HK-2 cells were subjected to *in vitro* transfection with oe-*ITCH*, sh-*ITCH*, or an empty vector using lentiviral infection. Following this, the cells were treated with 1 μ g/mL LPS for 24 h. Another subset of HK-2 cells was transfected with sh-*ITCH* or sh-NC, pretreated with 10 mM N-cetylcysteine (NAC) for 1 h, and treated with 1 μ g/mL LPS for 24 h. Furthermore, a separate subset of HK-2 cells was transfected with either an miR-214-3p inhibitor or NC inhibitor, in combination with sh-*ITCH* or sh-NC, for a duration of 48 h. A distinct subset of HK-2 cells underwent transfection with either sh-ABCA1 or sh-NC, alongside oe-*ITCH*, for a period of 48 h. Subsequently, cells were exposed to 1 μ g/mL LPS for 24 h.

2.4. Assessment of kidney function

Before euthanasia, serum samples were collected from mice. The evaluation of serum creatinine (Scr) and blood urea nitrogen (BUN) serum levels were determined using assay kits provided by the Nanjing Jiancheng Bioengineering Institute (China). Mouse urine samples were centrifuged at 2000 r/min for 20 min. The concentrations of neutrophil gelatinase-associated lipocalin (NGAL) and kidney injury molecule-1 (Kim-1) in the urine were determined using their respective ELISA kits: the mouse NGAL ELISA kit (ml002141, Mlbio, China) and the mouse Kim-1 ELISA kit (CSB-E08809m, CUSABIO, Wuhan, China).

2.5. Hematoxylin and eosin (H&E) staining

Kidney tissues were fixed with 10% formaldehyde, dehydrated with ethanol, and embedded in paraffin. Tissue sections were cut into 4 μ m slices. The sections were deparaffinized using xylene, rehydrated with ethanol, and stained with hematoxylin and eosin (C01055, Beyotime,

Nantong, China). Finally, the sections were blocked in neutral resin (G8590, Solarbio, Beijing, China) for observation under a light microscope (Olympus, Tokyo, Japan). The tubular injury was scored by quantifying the percentage of damaged tubules and categorized as follows: grade 0 (no damage), grade 1 (less than 25% damage), grade 2 (25–49% damage), grade 3 (50–75% damage), and grade 4 (more than 75% damage).

2.6. Periodic acid-Schiff (PAS) staining

For PAS staining, kidney tissue samples (1 mm³) were fixed in 10% formaldehyde at 4°C for 24 h. Following fixation, the samples were dehydrated in a graded ethanol series (30%, 50%, 70%, 80%, 95%, and 100%), embedded in paraffin, and sectioned at 5 µm. The sections were incubated for 10-min incubation with a periodate acid solution (C0142S, Beyotime, China). The sections were then placed in a shaker filled with distilled water and shaken for 5 min. Finally, the sections were dehydrated with ethanol and sealed with neutral resin for observation under a light microscope (Olympus, Japan).

2.7. Apoptosis assay

Apoptosis in kidney tissues was identified by TUNEL assay using the One Step TUNEL Apoptosis Assay Kit (C1082, Beyotime, China), as recommended by the supplier. Paraffin-embedded tissues were first deparaffinized using xylene and subsequently rehydrated through a graded ethanol series at room temperature. After washing with PBS, renal tissue sections were fixed in 1% paraformaldehyde for 15 min at room temperature. This was followed by a 30-minute treatment with 50 µL of proteinase K working solution at 37°C. The sections were then incubated with the TUNEL reaction mixture for 1 h at 37°C in the dark. Nuclei were stained with DAPI for 5 min at room temperature and sections were mounted using an anti-fade reagent (Solarbio, China). Imaging was conducted using an inverted fluorescence microscope (Olympus, Japan).

2.8. Luciferase reporter assay

The starBase version 2.0 platform (<https://starbase.sysu.edu.cn/starbase2/>) was utilized to predict the binding sites between circ-ITCH and miR-214-3p, as well as between miR-214-3p and ABCA1 [22]. Their interactions were validated using a luciferase reporter assay, as previously described [23].

2.9. Fluorescence in situ hybridization (FISH)

The Ribo FISH kit (RiboBio, China) was used to determine the localization of circ-ITCH in HK-2 cells. Initially, 4% paraformaldehyde (P0099-100 mL, Beyotime, China) was used to immobilize cells for 15 min, followed by 0.1% Triton X-100 digestion for an additional 15 min. After washing with PBS, cells were incubated in 2×sealing solution for 30 min at 37°C, after

which they were dehydrated using a graded ethanol series. The hybridization liquid containing probe (1 µg/mL targeting circ-ITCH) was denatured at 73 ± 1°C for 5 min. Next, cells were incubated with denatured probes targeting circ-ITCH at 37°C overnight in a wet cassette. After hybridization, the cover slide was discarded and then washed in 0.4 × SSC/0.3% Tween-20 at 65°C for 2 min, followed by a 2-min wash in 2×SSC/0.1% Tween-20 at room temperature. Nuclei were counterstained with DAPI, and images of the cells were captured using an UltraVIEW VoX Spinning Disk Confocal Microscope (PerkinElmer, Branford, CT).

2.10. Cell counting kit-8 (CCK-8) assay

The CCK-8 assay was performed on HK-2 cells in accordance with kit protocols (C0037, Beyotime, China).

2.11. Flow cytometry

To ascertain cellular apoptosis, HK-2 cells were seeded onto a six-well plate and subsequently subjected to enzymatic digestion using 0.25% trypsin (T1300, Solarbio, China). After centrifugation at 1500 rpm for 5 min, the cells were resuspended to a concentration of 1.0 × 10⁵ cells/mL. Following centrifugation, the cells were suspended in 195 µL of Annexin V-EGFP solution. The cell suspension was subjected to a 10-min period of darkness, followed by incubation with Annexin V-EGFP (5 µL) and propidium iodide (10 µL). Apoptosis was detected using a CytoFLEX flow cytometer (Beckman Coulter, Brea, CA).

2.12. Determination of reactive oxygen species (ROS) generation

As previously described, ROS levels in cells and kidney tissues were measured using 2',7'-dichlorodihydrofluorescein diacetate (H₂DCFDA) [24].

2.13. Enzyme-linked immunosorbent assay (ELISA)

The levels of ROS, malondialdehyde (MDA), and superoxide dismutase (SOD) in the kidney tissues and cells were determined using specific ELISA kits. Additionally, the concentrations of interleukin (IL)-1β, IL-6, and tumor necrosis factor (TNF-α) in both serum and cells were measured using corresponding ELISA assays. The ELISA kits used included: ROS assay kit (CA1410, Solarbio, China), mouse MDA kit (E-BC-K025-S, Elabscience, Houston, TX), mouse SOD ELISA kit (ml643059, mlbio, China), mouse IL-1β ELISA kit (ml301814, mlbio), mouse IL-6 ELISA kit (ml063160, mlbio), mouse TNF-α ELISA kit (ml002095, mlbio), human IL-1β ELISA kit (FHK0016, Jiamay Biotech, China), human IL-6 ELISA kit (ml058097, mlbio), and human TNF-α ELISA kit (ml077385, mlbio). The absorbance of MDA was set at 532 nm and that of SOD, IL-1β, IL-6, and TNF-α was set at 450 nm. The absorbance levels of these parameters were measured using a SpectraMax

M Series Multi-Mode Microplate Reader (Molecular Devices, Sunnyvale, CA).

2.14. Measurement of ROS levels in mitochondria

ROS levels in HK-2 cell mitochondria were measured using MitoSOX Red reagent (M36008, Thermo Fisher Scientific, Waltham, MA). The Cell Mitochondria Isolation Kit (C3606, Beyotime, China) was used to isolate mitochondria from HK-2 cells, and then the mitochondria were incubated with MitoSOX reagent (5 μ M) at 37°C for 10 min in the absence of light. Following three washes with D-hank solution, the mitochondria were observed using an Olympus CKX53 inverted microscope (Tokyo, Japan).

2.15. Evaluation of mitochondrial function

Mitochondrial function was evaluated by measuring both mitochondrial complex I activity and adenosine triphosphate (ATP) levels. The complexes I/II/III/IV activities of mitochondria in kidney tissues were determined using the electron transport chain complex I assay kit (A089-1-1), complex II assay kit (A089-2-1), complex III assay kit (A089-3-1), and complex IV assay kit (A089-4-1) (Nanjing Jiancheng Bioengineering Institute, China). The ATP Content Assay Kit (BC0300, Solarbio, China) was used to measure ATP levels.

2.16. Transmission electron microscopy

Glutaraldehyde (2.5%; P1126, Solarbio, China) was utilized to immobilize 1 mm³ of kidney tissue for 48h, followed by 2-h fixation with 1% OsO₄ (#18456, TED PELLA INC, Redding, CA). Following six washes with PBS and gradual dehydration with acetone, tissues were embedded in 3 mL of Epon812 resin for cutting into 60nm slices. Uranyl acetate and lead citrate staining were performed on the sections, which were then observed using a TEM (JEM-1011, JEOL, Tokyo, Japan).

2.17. Detection of mitochondrial membrane potential

The MMP of cells was monitored using the MMP assay kit with JC-1 (C2006, Beyotime, China) and flow cytometry following the user manual.

2.18. Measurement of oxygen consumption rate

OCR in HK-2 cells was assessed utilizing a Seahorse XF analyzer and a Seahorse XF Cell Mito Stress Test kit (Agilent, Palo Alto, CA). The cells were resuspended in Seahorse XF DMEM containing 10mM glucose, 1mM sodium pyruvate, and 2mM L-glutamine, and subsequently seeded onto Cell-Tak coated XFe96 microplates. Prior to the assay, cells underwent a 1-h equilibration in a non-CO₂ incubator at 37°C. During the assay, a sequential injection of mitochondrial inhibitors – 1.5 μ M oligomycin, 0.5 μ M FCCP, and 0.5 μ M rotenone/antimycin A – was administered to each well. OCR

Table 1. Primer sequences.

Gene	Sequences (5'–3')
Mouse DRP-1	Forward: TGCCATCGTGAAGAAGTGCC Reverse: CATCCCTTGCTACCCGAGC
Human DRP-1	Forward: TCAAGCAGCAGAAGGTGGAG Reverse: TCGTGAGCCAGACCAAAGTC
Mouse OPA-1	Forward: GCTGAGCGTGCTTATCAACG Reverse: AGGCCTCAGGTGGGTATGAT
Human OPA-1	Forward: AAGCCAGTCTGACAATGGG Reverse: ACGTTGACTTGGCTGTAGGG
Mouse ABCA1	Forward: GCAGAACTGGGAGTCTGTCTC Reverse: CATCGATGGTCAGCGTGCA
Human ABCA1	Forward: GCTGGTGTGGACCTTACTC Reverse: GCAGTTCATATGGCAGCAC
Mouse GAPDH	Forward: TGTGGGCATCAATGGATTGG Reverse: ACACCATGTATTCCGGGTCAAT
Human GAPDH	Forward: GTCAAGGCTGAGAACGGGAA Reverse: AAATGAGCCCCAGCCTTCTC
Human circ-ITCH	Forward: AGCAATGCAGCAGTTT Reverse: TGTAGCCCATCAAGACA
Mouse miR-214-3p	Forward: CGTTAACAGCTGTACCATC Reverse: AGTGATGGTGTAGGTGAGG
Human miR-214-3p	Forward: TGGAGTTGGGGTTTCTGTGA Reverse: TTCAGTGCACAGGTTCGAAGC
Mouse U6	Forward: AAGACAGCGCAGAATCACCC Reverse: CTCACCAGATGCCCGTTGTA
Human U6	Forward: GATGAGTCCGAGGACGGGAT Reverse: GAACCACACTCTGGGACAGG
Human D-Loop 2	Forward: CTGTCTTTGATTCTCGCTCAT Reverse: GTGGCTGTGCAGACATTCAA
Human G6PC	Forward: GGCTCTCAACTCCAGCATGT Reverse: AGGACGAGGGAGGCTACAAT

data interpretation was carried out using the Seahorse Wave 2.6.1 Software.

2.19. RT-qPCR

TRIzol reagent was used to extract total RNAs from both the kidney tissues and cells. RT-qPCR was performed as previously described [25]. The primers used are listed in Table 1.

2.20. Quantification of mitochondrial DNA (mtDNA)

Total DNA was harvested from treated cells using FastPure Cell/Tissue DNA Isolation Mini Kit (DC102-01, Vazyme, Nanjing, China). The mtDNA copy number was expressed as the mtDNA/nuclear DNA (nDNA) ratio. Mitochondrial gene D-Loop 2 (mtDNA) and nuclear gene G6PC (nDNA) were determined by RT-qPCR. Primers are listed in Table 1.

2.21. Western blotting

Total proteins were extracted from the kidney tissues and cells. Western blotting was performed as previously described [26]. The primary antibodies used were cleaved casepase-3 antibody (1:1000; AF7022, Affinity, Queen City, TX), Bax antibody (1:1000; AF0120, Affinity), Bcl-2 antibody (1:1000; AF6139, Affinity), anti-DRP-1 antibody (1:1000; ab184247, Abcam, Cambridge, UK), OPA-1 Rabbit mAb (1:1000; #80471, CST, Danvers, MA), anti-MFN-1 antibody (1:1000; ab221661, Abcam), HSP60 antibody (1:1000; AF5374, Affinity), SDHA antibody (1:1000; DF7043, Affinity), PINK1 antibody (1:1000;

DF7742, Affinity), Parkin antibody (1:1000; AF0235, Affinity), LC3B antibody (1:1000; AF4650, Affinity), ABCA1 Rabbit mAb (1:200; #96292, CST), and GAPDH Rabbit mAb (1:1000; #5174, CST). The secondary antibody used was Goat Anti-Rabbit IgG H&L (HRP) (1:2000; ab205718, Abcam, UK). Relative protein levels were calculated by normalizing to GAPDH.

2.22. Statistical analyses

Each individual experiment was conducted in triplicate. Data are presented as the mean \pm standard error of the mean (s.e.m.). Statistical analyses were conducted using GraphPad Prism version 7.0, La Jolla, CA, wherein one-way ANOVA and Student's *t*-test were used to assess the disparities among the groups. A value of $p < 0.05$ was considered statistically significant.

3. Results

3.1. Circ-ITCH improves mitochondrial dysfunction in sepsis-induced AKI mice

To study the role of circITCH in sepsis-induced AKI, a xenograft mouse model of sepsis was constructed by LPS induction. SCr and BUN are critical indicators of renal function. As presented in Figure S1(A), SCr and BUN levels were higher in the serum of LPS-induced sepsis mice ($p < 0.01$). The histological appearance of kidney tissues from the control mice was compared to that of the LPS-induced sepsis mice. H&E and PAS staining revealed that LPS-induced sepsis mice had severe histological kidney injuries, as evidenced by inflammatory cell infiltration, renal tubule epithelial cell vacuolar degeneration, and detachment (Figure S1(B)). The tubular injury score in the renal cortex of the LPS-induced sepsis mice was higher than that in the renal cortex of the control mice ($p < 0.01$, Figure S1(A)). Apoptosis was observed in the kidney tissues of these mice. As displayed in Figure S1(C), LPS-induced sepsis mice had more apoptotic cells than the control mice. In addition, there was a significant elevation in biomarkers of oxidative stress (ROS and MDA) and inflammation (IL-1 β , IL-6, and TNF- α) in the kidney tissues of LPS-induced sepsis mice ($p < 0.01$, Figure S1(D and E)). On the other hand, SOD levels, representing an antioxidant enzyme, were diminished in septic mice ($p < 0.01$, Figure S1(E)). The ATP levels and the activity of mitochondrial complexes I, II, III, and IV are indicators of mitochondrial function. The ATP production in the kidney tissues was significantly reduced in LPS-induced sepsis mice ($p < 0.01$). In LPS-induced sepsis mice, the activity of complexes I/II/III/IV in the mitochondria was decreased by nearly two-fold relative to that in control mice ($p < 0.01$, Figure S2(A)). Additionally, TEM revealed that the mitochondria in the kidney tubular cells of LPS-induced sepsis mice exhibited more severe injury than in the control mice, with evident mitochondrial fragmentation, swelling, and loss of cristae (Figure S2(B)). Expressions of the mitochondrial fission protein (DRP-1) and fusion proteins (OPA-1 and MFN-1) were also examined. The results showed

that DRP-1 expression was upregulated, and levels of OPA-1 and MFN-1 were downregulated in LPS-induced sepsis mice ($p < 0.01$, Figure S2(C and D)). These data indicated that mitochondrial dysfunction is a predominant characteristic of sepsis-induced AKI.

Subsequently, circ-ITCH was identified as a downregulated circRNA in LPS-induced sepsis mice ($p < 0.01$, Figure S3(A)). Thus, circ-ITCH was overexpressed in LPS-induced sepsis mice to further investigate its role in the regulation of mitochondrial function. Circ-ITCH expression was significantly upregulated in the LPS-induced sepsis mice transfected with oe-ITCH, compared to the oe-NC mice ($p < 0.01$, Figure S3(A)). Compared to oe-NC, the administration of oe-ITCH resulted in a decrease in the serum levels of SCr and BUN in the LPS-induced sepsis mice ($p < 0.05$, Figure 1(A)). The levels of NGAL and Kim-1 (AKI-associated markers) in the urine of LPS-induced sepsis mice were also significantly decreased by circ-ITCH overexpression ($p < 0.01$, Figure 1(B)). H&E and PAS staining indicated that oe-ITCH ameliorated kidney injury and pathological damage, as evidenced by decreased inflammatory cell infiltration and renal interstitial edema (Figure 1(C and D)). Moreover, oxidative stress and inflammation in the model mice were alleviated by oe-ITCH treatment ($p < 0.05$, Figure 1(E and F)). Post oe-ITCH treatment, a decline in apoptosis in kidney tissues was also noticed by TUNEL assay ($p < 0.01$, Figure S3(B)). We also discovered that overexpression of ITCH led to a downregulation in the expression of pro-apoptotic markers, such as cleaved caspase-3 and Bax, and an upregulation of the anti-apoptotic marker, Bcl-2 ($p < 0.01$, Figure S3(C)). Our findings demonstrate that oe-ITCH notably enhanced the ATP content and the activities of mitochondrial complexes I/II/III/IV when compared to the oe-NC group ($p < 0.01$, Figure 2(A)). TEM findings demonstrated a reduction in mitochondrial swelling in kidney tissues of mice treated with oe-ITCH as opposed to those with oe-NC (Figure 2(B)). Next, we found an increase in mtDNA copy number in LPS-induced sepsis mice after oe-ITCH transfection ($p < 0.01$, Figure 2(C)). Furthermore, after oe-ITCH transfection in LPS-induced sepsis mice, the expression levels of DRP-1 decreased, while those of OPA-1 and MFN-1 increased ($p < 0.01$, Figure 2(D and E)). Also, oe-ITCH downregulated the expression of mitochondria-related proteins (HSP60 and SDHA) ($p < 0.01$, Figure 2(E)). Besides, a study indicated that sepsis-AKI is associated with PINK-parkin-induced mitophagy [9]. We found that oe-ITCH reduced the expression of PINK-parkin-induced mitophagy-related proteins (PINK1, Parkin, and LC3II/LC3I) ($p < 0.01$, Figure S4).

3.2. Circ-ITCH prevents apoptosis and mitochondrial dysfunction in LPS-stimulated HK-2 cells

To further substantiate the influence of circ-ITCH on sepsis-induced AKI, elicitation of a sepsis cell model in HK-2 cells was accomplished *via* LPS stimulation. Circ-ITCH was overexpressed and knocked down in model cells by transfecting oe-ITCH and sh-ITCH, respectively. As expected,

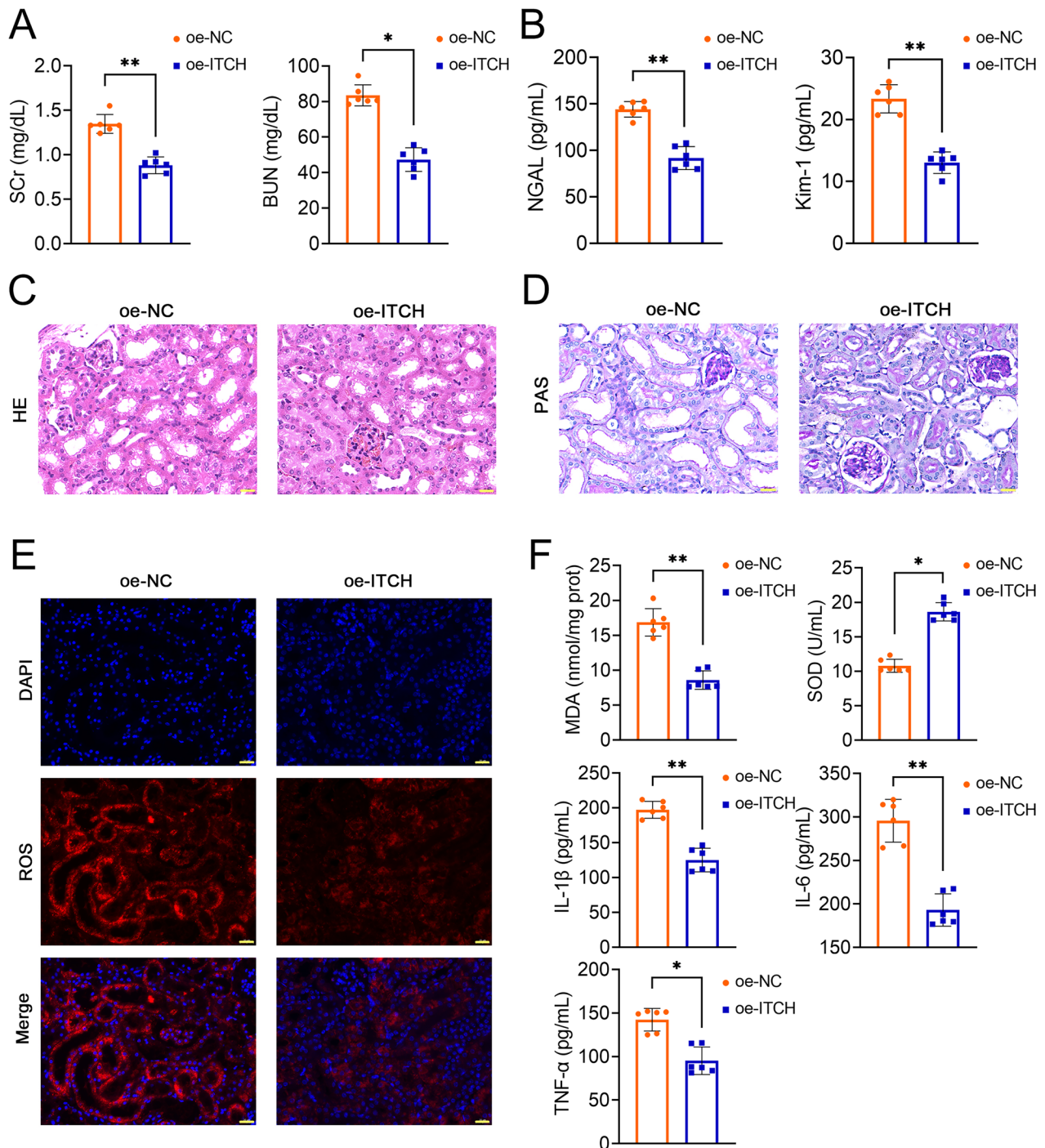


Figure 1. Circ-ITCH overexpression alleviates kidney injury, oxidative stress, and inflammation in lipopolysaccharide (LPS)-induced sepsis mice. (A) Levels of serum creatinine (SCr) and blood urea nitrogen (BUN) were detected by corresponding kits. (B) Levels of neutrophil gelatinase-associated lipocalin (NGAL) and kidney injury molecule-1 (Kim-1) in the urine of mice were detected by ELISA kits. (C,D) Hematoxylin and eosin (H&E) and periodic acid-Schiff staining were used to determine kidney injury (scale bar = 20 μ m). (E) H_2DCFDA probe was used to detect the reactive oxygen species (ROS) level in kidney tissues of LPS-induced sepsis mice (scale bar = 20 μ m). (F) Levels of malondialdehyde (MDA), and superoxide dismutase (SOD) in kidney tissues and interleukin (IL)-1 β , IL-6, and tumor necrosis factor (TNF)- α in serum were detected by corresponding ELISA kits. LPS-induced sepsis mice were transfected with oe-negative control (NC) or oe-ITCH (ITCH overexpression). * $p < 0.05$, ** $p < 0.01$.

circ-ITCH expression decreased in HK-2 cells stimulated with LPS ($p < 0.05$). Oe-ITCH and sh-ITCH increased and decreased circ-ITCH expression, respectively, in HK-2 cells stimulated by LPS, indicating successful transfection ($p < 0.05$, Figure 3(A)). The results showed that the proliferation and apoptosis of HK-2 cells stimulated by LPS were reduced and increased,

respectively, compared to those of control cells ($p < 0.01$). Circ-ITCH overexpression enhanced proliferation and suppressed apoptosis of LPS-stimulated HK-2 cells ($p < 0.01$, Figure 3(B,C)). Evidence of augmented oxidative stress and inflammation in cells was observed following LPS stimulation ($p < 0.01$). Our results showed that circ-ITCH overexpression

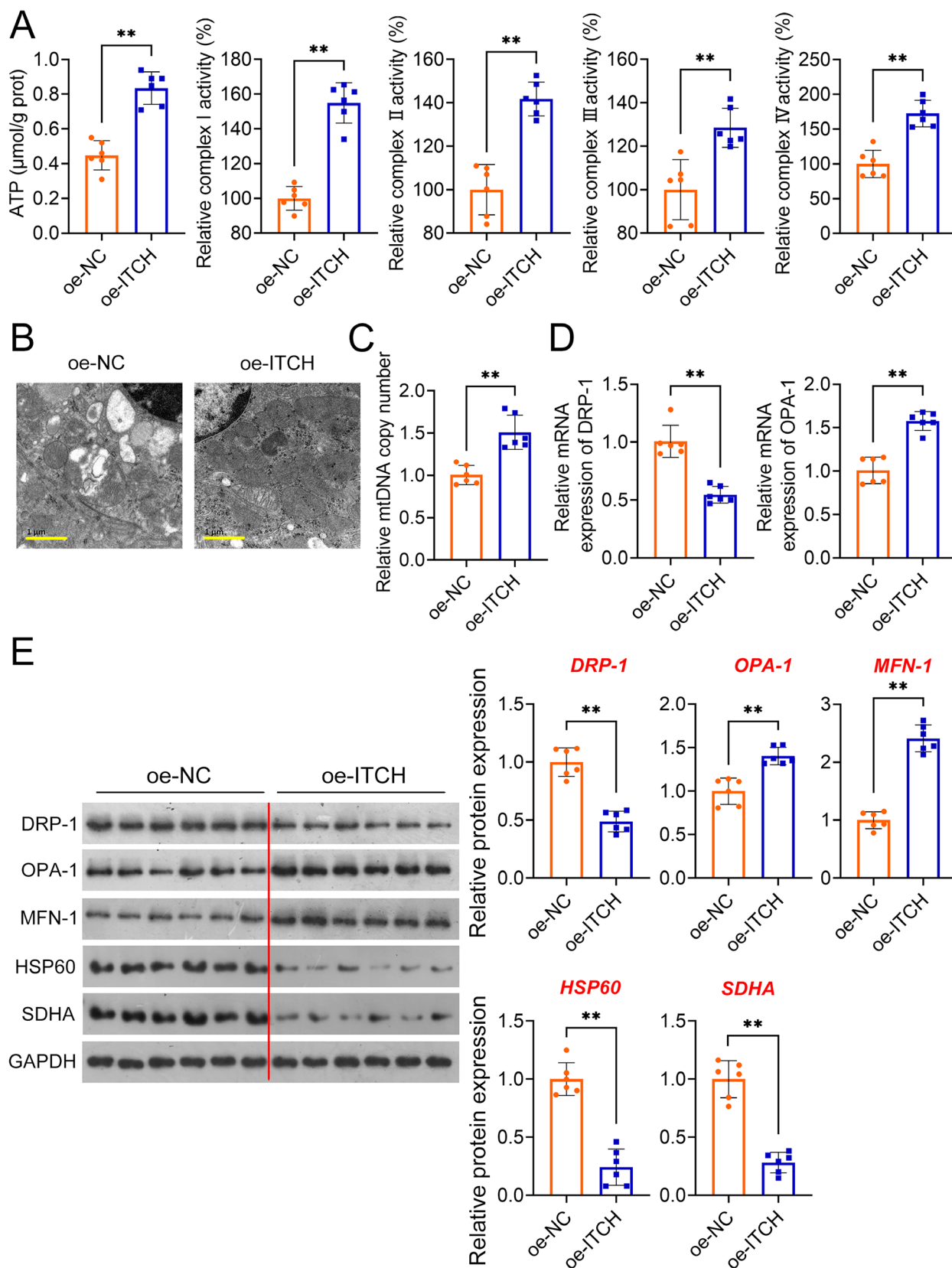


Figure 2. Circ-ITCH protects mitochondrial function of kidney tissues in lipopolysaccharide (LPS)-induced sepsis mice. (A) Adenosine triphosphate (ATP) levels and mitochondrial complexes I/II/III/IV activities in kidney tissues was determined using the corresponding assay kits. (B) Transmission electron microscopy was used to identify mitochondrial morphology in kidney tissues (scale bar = 1 μm). (C-D) RT-qPCR was used to determine the mtDNA copy number and the relative expression of DRP-1 and OPA-1 in kidney tissues. (E) Western blotting was used to measure the expression of DRP-1, OPA-1, MFN-1, HSP60, and SDHA in kidney tissues. LPS-induced sepsis mice were transfected with oe-negative control (NC) or oe-ITCH (ITCH overexpression). ** $p < 0.01$.

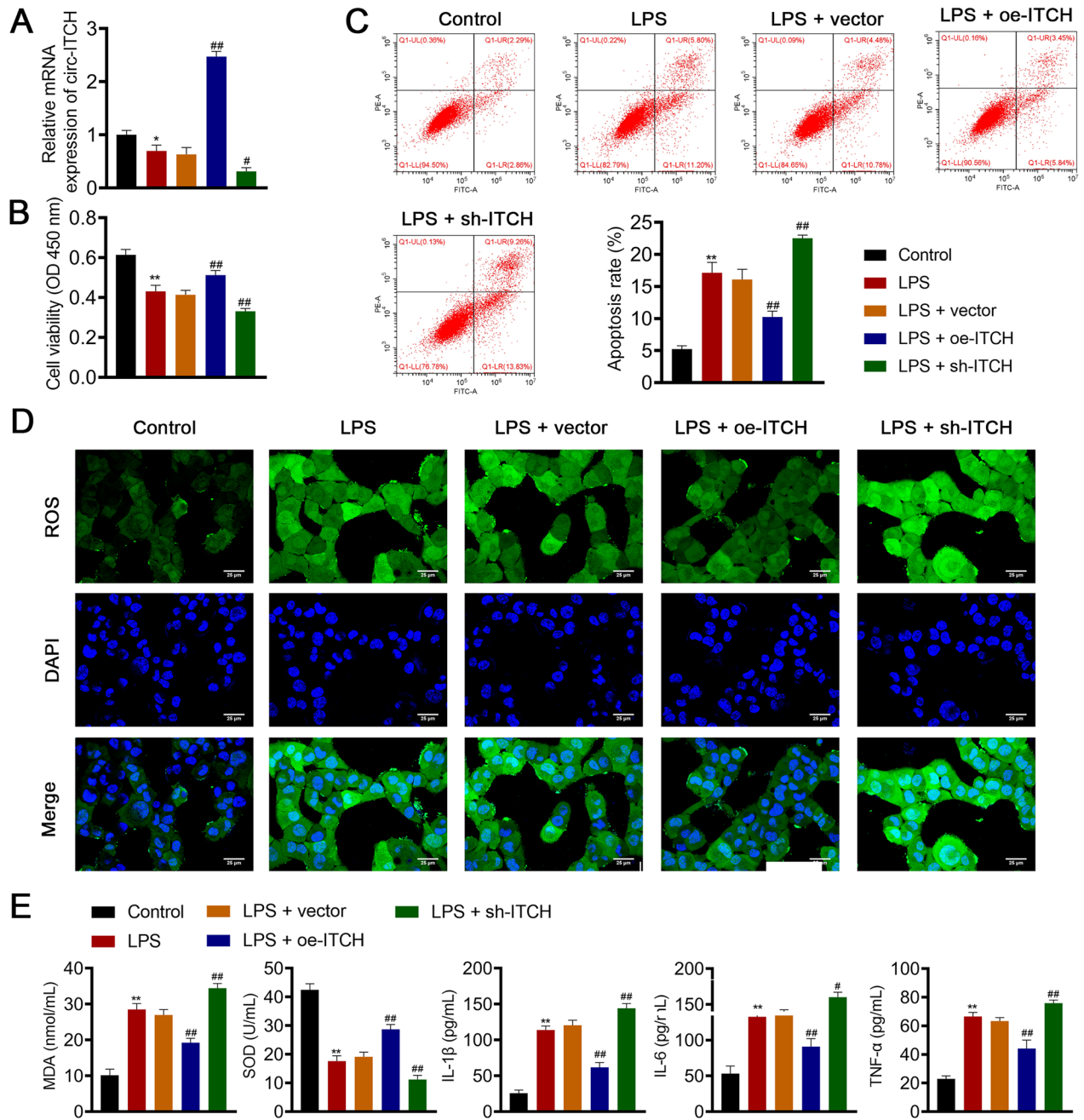


Figure 3. Circ-ITCH prevents apoptosis and inflammation in lipopolysaccharide (LPS)-stimulated HK-2 cells. (A) RT-qPCR was used to determine the relative expression of circ-ITCH in cells. (B) CCK-8 assay was used to detect cell viability. (C) Flow cytometry was used to identify cell apoptosis. (D) H_2DCFDA probe was used to detect the reactive oxygen species (ROS) level in cells (scale bar = 25 μm). (E) Levels of malondialdehyde (MDA), superoxide dismutase (SOD), interleukin (IL)-1 β , IL-6, and tumor necrosis factor (TNF)- α in cells were detected by corresponding ELISA kits. * $p < 0.05$, ** $p < 0.01$ vs. control; # $p < 0.05$, ## $p < 0.01$ vs. LPS + vector.

led to a decrease in oxidative stress and inflammatory response in LPS-stimulated HK-2 cells ($p < 0.05$, Figure 3(D,E)), whereas circ-ITCH knockdown had the opposite effect. In LPS-stimulated HK-2 cells, we also observed mitochondrial dysfunction. This was evidenced by decreased levels of OCR, OPA-1, and MFN-1, along with an increase in DRP-1 levels ($p < 0.01$). Overexpression of circ-ITCH mitigated mitochondrial dysfunction, while its knockdown exacerbated it in LPS-stimulated HK-2 cells ($p < 0.05$, Figure 4(A–C)).

3.3. Circ-ITCH ameliorates mitochondrial dysfunction induced by oxidative stress in LPS-stimulated HK-2 cells

The influence of circ-ITCH on oxidative stress-induced mitochondrial dysfunction was further investigated by NAC and/or sh-ITCH treatment of LPS-stimulated HK-2 cells. NAC is a ROS scavenger that can effectively inhibit oxidative stress [2]. As shown in Figure 5(A), ROS and MDA levels decreased, and SOD levels increased in HK-2 cells stimulated by LPS and NAC ($p < 0.01$). The mitochondrial ROS levels also

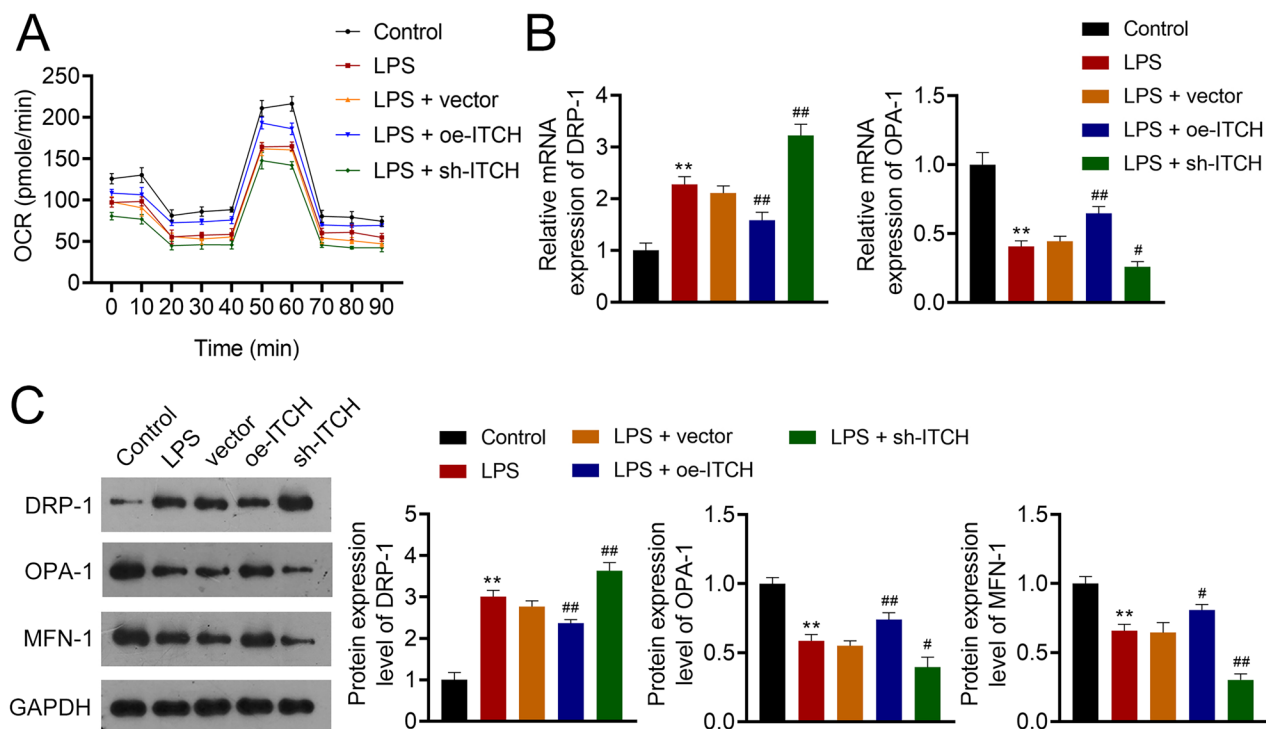


Figure 4. Circ-ITCH alleviates mitochondrial dysfunction in lipopolysaccharide (LPS)-stimulated HK-2 cells. (A) OCR was detected in cells. (B) RT-qPCR was used to determine the relative expression of DRP-1 and OPA-1 in cells. (C) Western blotting was used to measure the expression of DRP-1, OPA-1, and MFN-1 in cells. LPS-stimulated HK-2 cells were transfected with oe-ITCH (ITCH overexpression) or sh-ITCH (ITCH knockdown). ** $p < 0.01$ vs. control; # $p < 0.05$, ## $p < 0.01$ vs. LPS+vector.

showed a decreasing trend in the NAC group (Figure 5(B)). However, ITCH knockdown aggravated oxidative stress in cells of the NAC group ($p < 0.05$, Figure 5(A and B)). Moreover, MMP in the cells was elevated by NAC treatment, whereas sh-ITCH promotes the loss of MMP in the NAC group ($p < 0.01$, Figures 5(C) and 6(A)). Additionally, NAC administration decreased the amount of DRP-1 and augmented the levels of OPA-1 and MFN-1 in LPS-activated HK-2 cells ($p < 0.01$). Similarly, ITCH knockdown inhibited the mitigating effect of NAC on LPS-induced mitochondrial dysfunction in HK-2 cells ($p < 0.05$, Figure 6(B and C)).

3.4. Circ-ITCH targets miR-214-3p/ABCA1 axis in LPS-stimulated HK-2 cells

FISH assay revealed that circ-ITCH is present in both the nuclei and cytoplasm of HK-2 cells (Figure 7(A)), suggesting that it functions as a molecular sponge for gene expression regulation. Circ-ITCH was predicted to bind miR-214-3p (Figure 7(B)). The interaction between circ-ITCH and miR-214-3p was confirmed ($p < 0.01$, Figure 7(C)). Additionally, bioinformatic analysis to predict that miR-214-3p targeted ABCA1 ($p < 0.01$, Figure 7(D and E)). MiR-214-3p and ABCA1 expression were evaluated. The results presented that miR-214-3p and ABCA1 expression was upregulated and downregulated, respectively, in LPS-induced sepsis mice ($p < 0.01$, Figure 7(F–H)). Circ-ITCH overexpression downregulated miR-214-3p levels and increased ABCA1 levels in LPS-induced sepsis mice ($p < 0.01$, Figure 7(F–H)).

3.5. Circ-ITCH alleviates mitochondrial dysfunction of LPS-stimulated HK-2 cells by targeting miR-214-3p/ABCA1 axis

Using an LPS-stimulated HK-2 cell model of AKI, we further confirmed that circ-ITCH protects against sepsis-induced AKI by targeting the miR-214-3p/ABCA1 axis. As shown in Figure 8(A and B), the miR-214-3p inhibitor enhanced the viability and reduced the apoptosis of HK-2 cells stimulated by LPS ($p < 0.01$). In addition, the miR-214-3p inhibitor alleviated oxidative stress (decreased ROS and MDA, as well as increased SOD) and the inflammatory response in HK-2 cells stimulated by LPS ($p < 0.01$, Figure 8(C and D)). For mitochondrial function, the miR-214-3p inhibitor downregulated DRP-1 expression and upregulated OPA-1 and MFN-1 levels ($p < 0.01$, Figure 8(E and F)). The protective effects of the miR-214-3p inhibitor on HK-2 cells stimulated by LPS were hindered by the knockdown of Circ-ITCH ($p < 0.05$, Figure 8(A–F)). Finally, RT-qPCR showed that an miR-214-3p inhibitor upregulated ABCA1 expression, but did not influence circ-ITCH levels in HK-2 cells stimulated by LPS ($p < 0.01$). The addition of sh-ITCH reduced circ-ITCH and ABCA1 expression and increased miR-214-3p levels ($p < 0.05$, Figure 8(G)).

Furthermore, we investigated the regulatory interplay between circ-ITCH and ABCA1 in LPS-stimulated HK-2 cells. The knockdown of ABCA1 counteracted the upregulatory effect of oe-ITCH on ABCA1 expression ($p < 0.01$, Figure 9(A)). Functionally, in LPS-stimulated HK-2 cells transfected with oe-ITCH, the serum levels of IL-1 β , IL-6, and TNF- α were notably elevated upon ABCA1 deficiency ($p < 0.01$, Figure 9(B)).

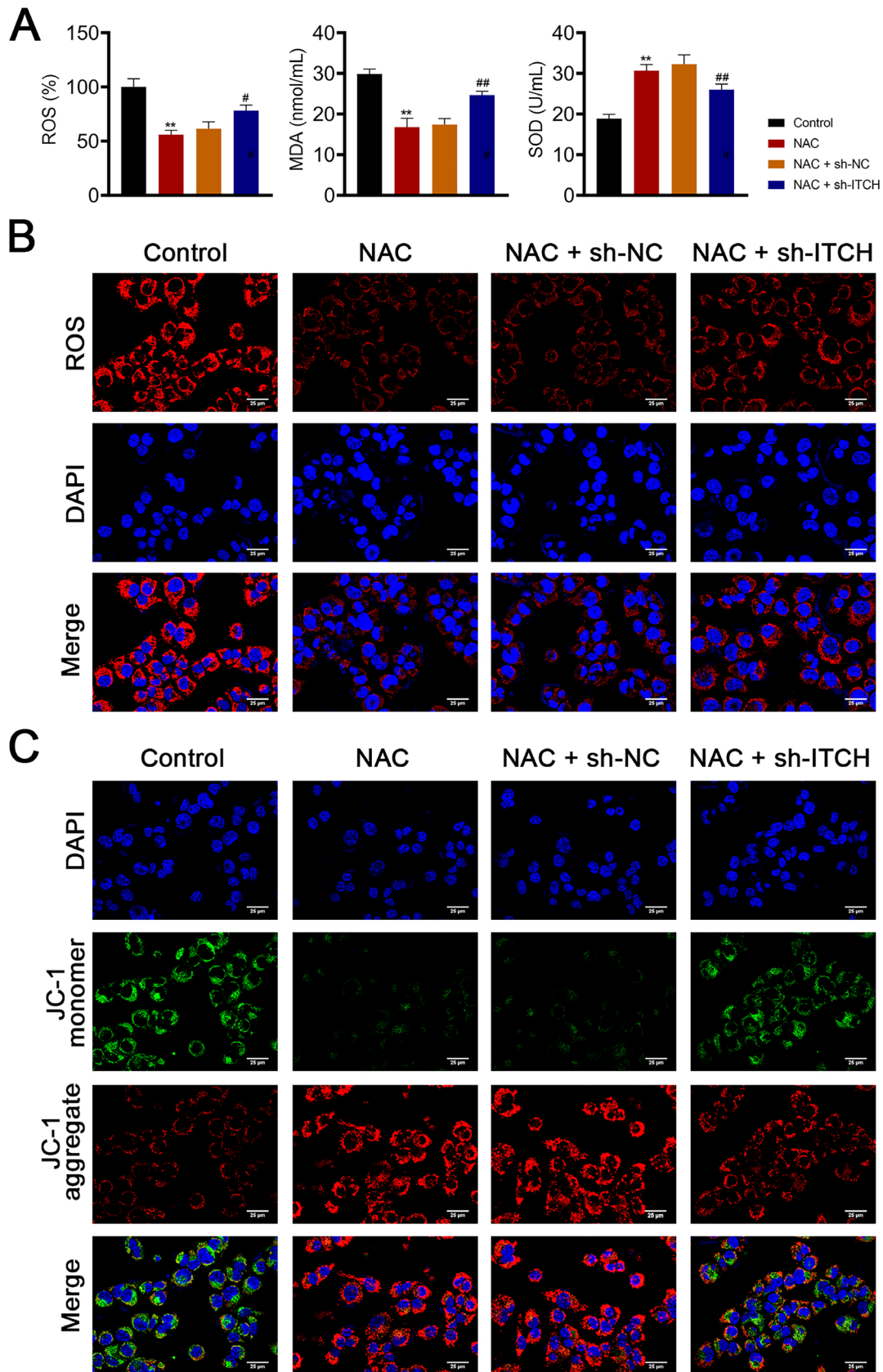


Figure 5. Circ-ITCH ameliorates mitochondrial dysfunction induced by oxidative stress in lipopolysaccharide (LPS)-stimulated HK-2 cells. (A) Levels of reactive oxygen species (ROS), malondialdehyde (MDA), and superoxide dismutase (SOD) in cells were detected by corresponding ELISA kits. (B) MitoSOX Red reagent was used to measure mitochondrial ROS in cells (scale bar = 25 μ m). (C) Mitochondrial membrane potential of cells was monitored using JC-1 staining (scale bar = 25 μ m). LPS-stimulated HK-2 cells were pretreated with N-cetylcysteine (NAC; a ROS scavenger) and transfected with sh-ITCH or sh-NC. ** $p < 0.01$ vs. control; # $p < 0.05$, ## $p < 0.01$ vs. NAC + sh-NC.

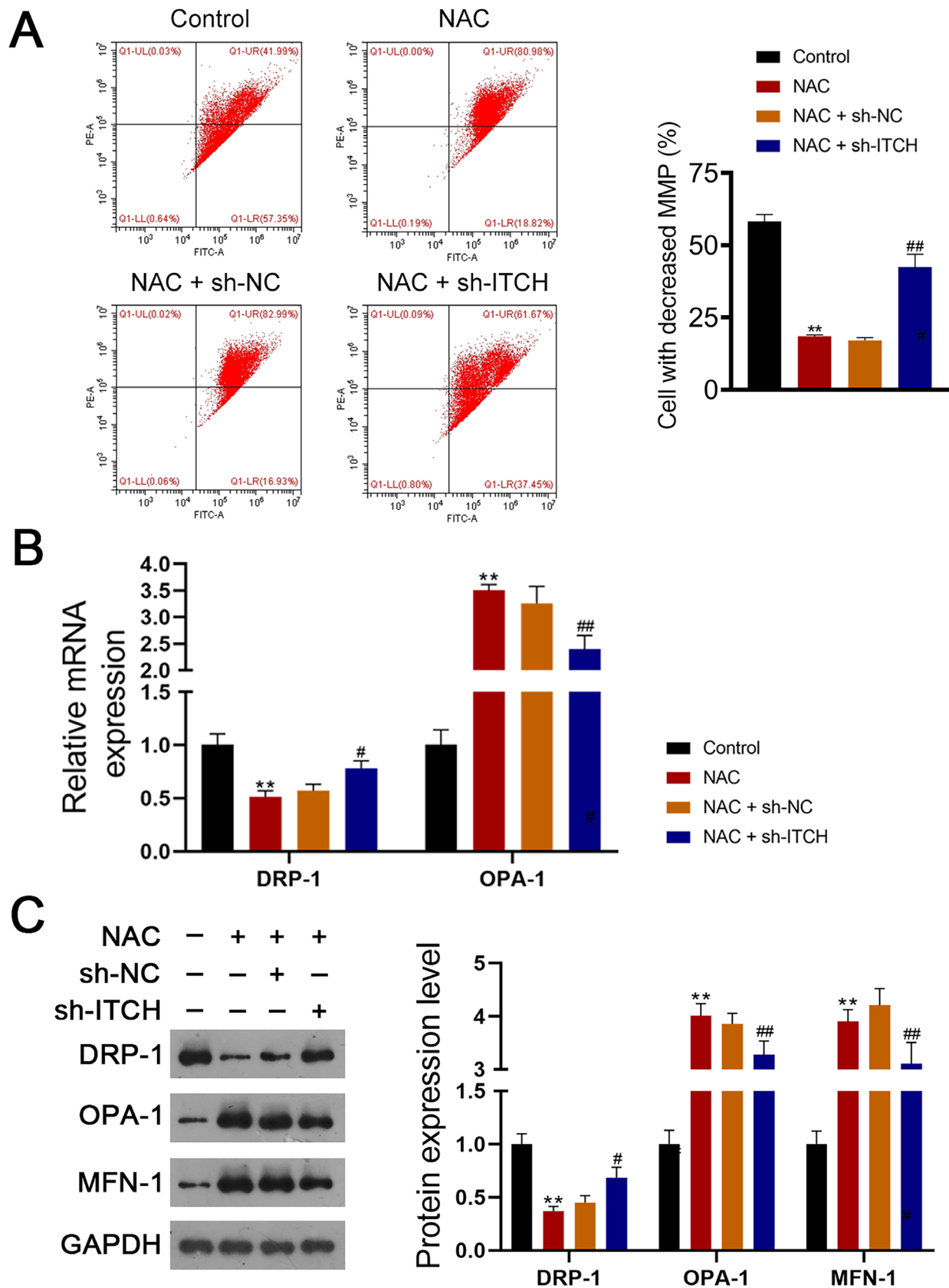


Figure 6. Circ-ITCH protects mitochondrial dysfunction induced by oxidative stress in lipopolysaccharide (LPS)-stimulated HK-2 cells. (A) Mitochondrial membrane potential (MMP) of cells was monitored using flow cytometry. (B) RT-qPCR was used to determine the relative expression of DRP-1 and OPA-1 in cells. (C) Western blotting was used to measure the expression of DRP-1, OPA-1, and MFN-1 in cells. LPS-stimulated HK-2 cells were pretreated with N-cetylcysteine (NAC; a ROS scavenger) and transfected with sh-ITCH or sh-NC. ** $p < 0.01$ vs. control; # $p < 0.05$, ## $p < 0.01$ vs. NAC+sh-NC.

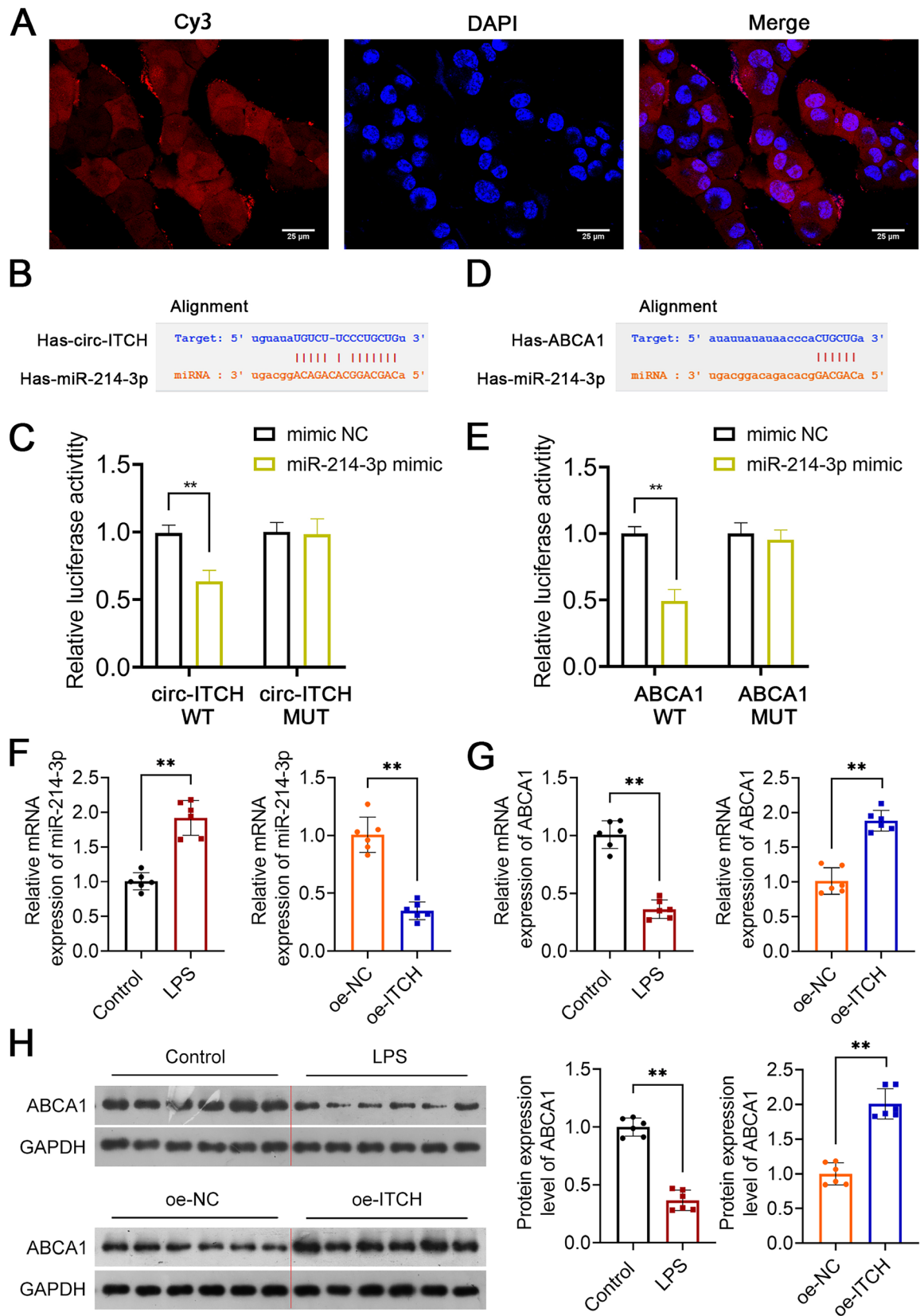


Figure 7. Circ-ITCH targets miR-214-3p/ABCA1 axis. (A) Circ-ITCH was identified to Localize to both nuclei and cytoplasm in HK-2 cells by fluorescence *in situ* hybridization (FISH) assay (scale bar = 25 μ m). (B, C) the interaction between circ-ITCH and miR-214-3p was predicted using the starBase v2.0 database and identified by dual-luciferase reporter assay. (D, E) The interaction between miR-214-3p and ABCA1 was predicted using the starBase v2.0 database and identified by dual-luciferase reporter assay. (F, G) RT-qPCR was used to determine the relative expression of miR-214-3p and ABCA1 in kidney tissues of lipopolysaccharide (LPS)-induced sepsis mice with/without oe-ITCH transfection. (H) Western blotting was used to measure the expression of ABCA1 in LPS-induced sepsis mice. ** $p < 0.01$.

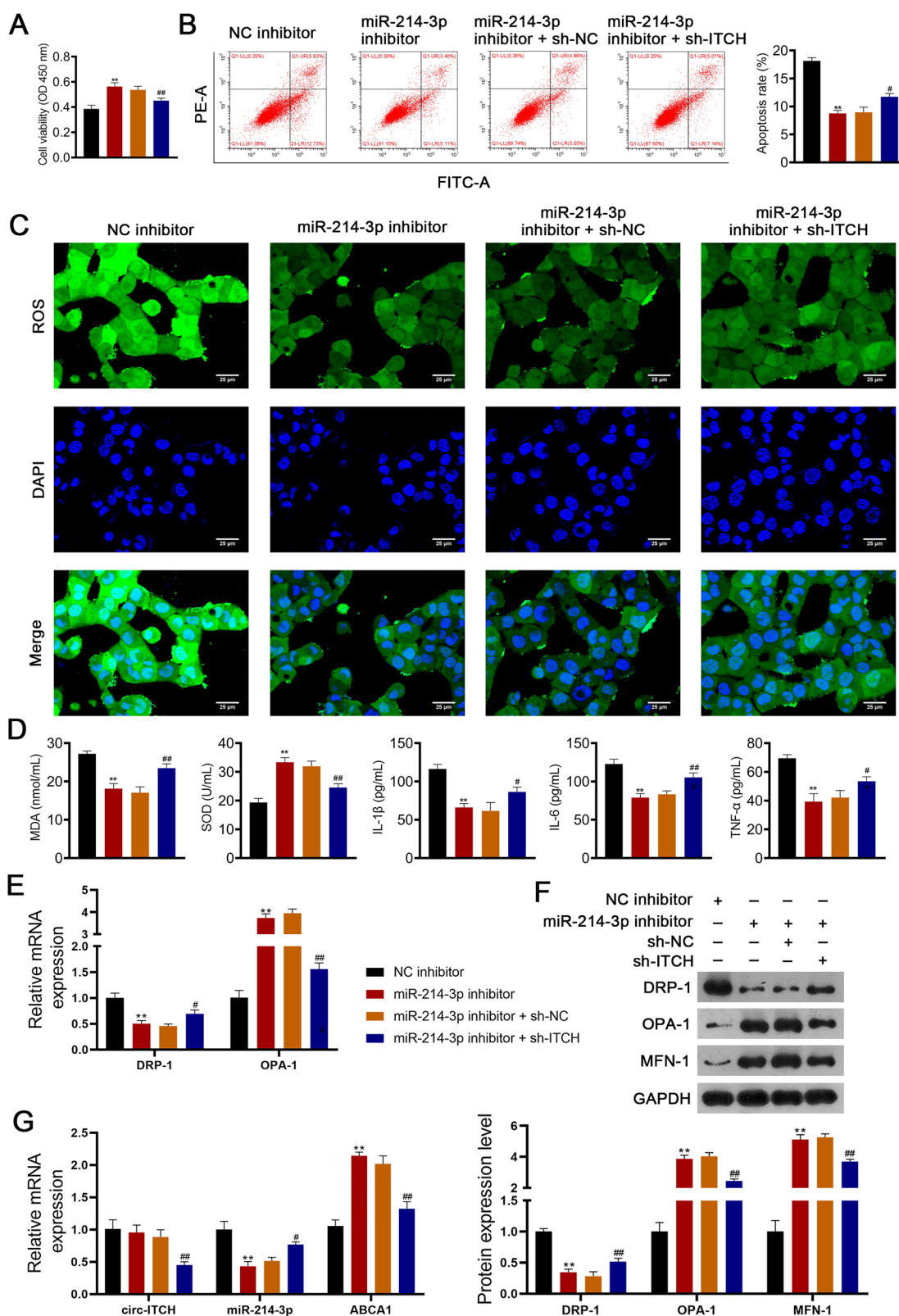


Figure 8. Circ-ITCH alleviates mitochondrial dysfunction of lipopolysaccharide (LPS)-stimulated HK-2 cells by targeting miR-214-3p/ABCA1 axis. (A) CCK-8 assay was used to detect cell viability. (B) Flow cytometry was used to identify cell apoptosis. (C) H_2DCFDA probe was used to detect the reactive oxygen species (ROS) level in cells (scale bar = 25 μm). (D) Levels of malondialdehyde (MDA), superoxide dismutase (SOD), interleukin (IL)-1 β , IL-6, and tumor necrosis factor (TNF)- α in cells were detected by corresponding ELISA kits. (E) RT-qPCR was used to determine the relative expression of DRP-1 and OPA-1 in cells. (F) Western blotting was used to measure the expression of DRP-1, OPA-1, and MFN-1 in cells. (G) LPS-stimulated HK-2 cells were transfected with miR-214-3p inhibitor or/and sh-ITCH. ** $p < 0.01$ vs. NC inhibitor; # $p < 0.05$, ## $p < 0.01$ vs. miR-214-3p inhibitor+sh-NC.

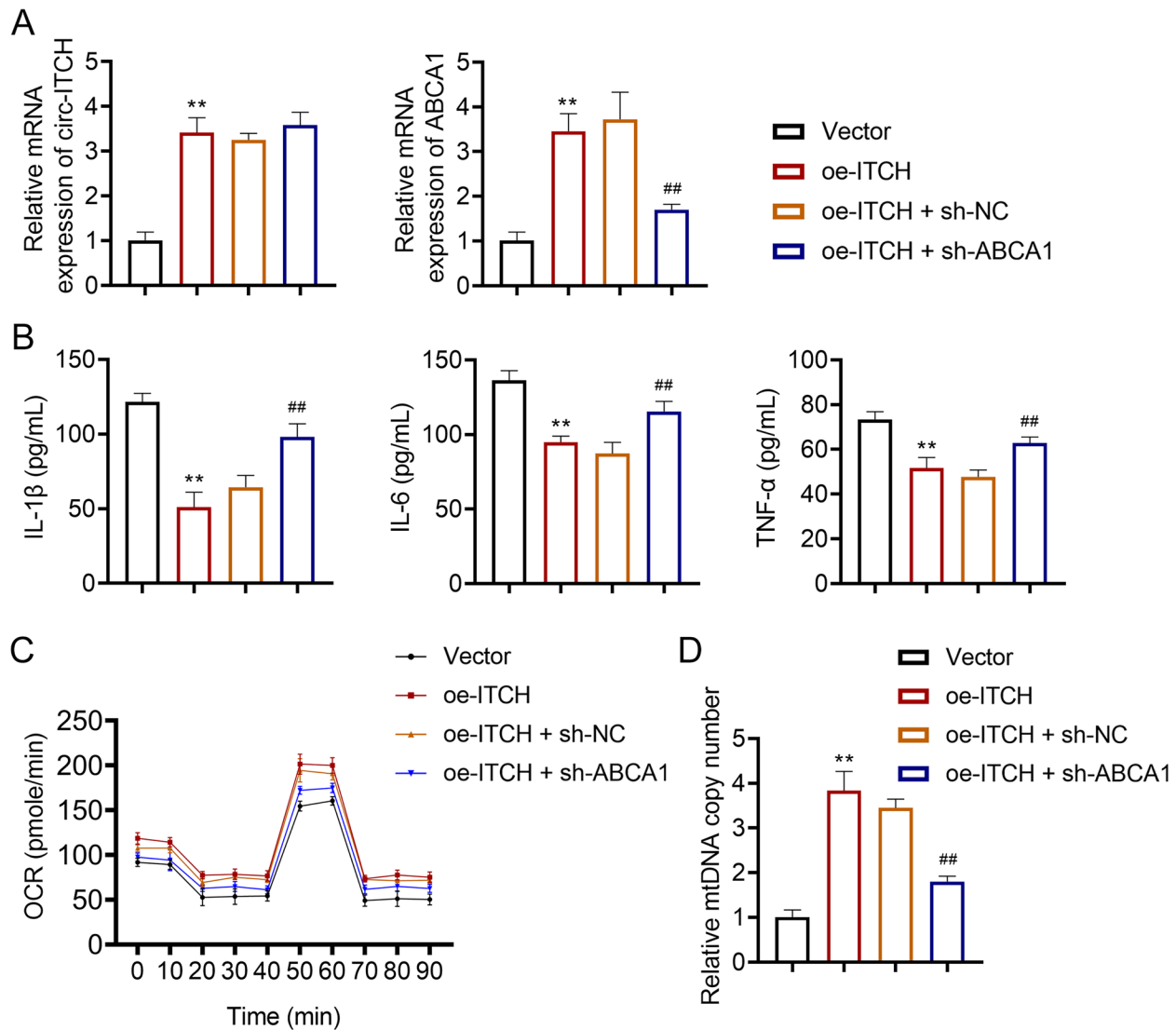


Figure 9. Regulatory interplay between circ-ITCH and ABCA1 in LPS-stimulated HK-2 cells. (A) RT-qPCR was used to determine the relative expression of circ-ITCH and ABCA1 in cells. (B) Levels of interleukin (IL)-1 β , IL-6, and tumor necrosis factor (TNF)- α in cells were detected by corresponding ELISA kits. (C) OCR was detected in cells. (D) RT-qPCR was used to determine the mtDNA copy number in cells. ** $p < 0.01$ vs. vector; *** $p < 0.01$ vs. oe-ITCH+sh-NC.

Additionally, in LPS-stimulated HK-2 cells, the knockdown of ABCA1 negated the enhancing effects of oe-ITCH on OCR levels and mtDNA copy number ($p < 0.01$, Figure 9(C and D)).

4. Discussion

Sepsis is an inflammatory response caused by a microbial infection that triggers dysfunction of multiple organs, including AKI [27]. Sepsis-associated AKI contributes to high morbidity and mortality [28]; therefore, early diagnosis is pivotal for sepsis treatment. CircRNAs are becoming novel potential biomarkers and therapeutic targets for diseases because of their widespread distribution and regulation of gene expression [28]. Circ-ITCH, a novel circRNA, is a well-known tumor suppressor [13]. In recent years, the pathological role of circ-ITCH in non-neoplastic diseases has been gradually explored [13]. A previous study reported that circ-ITCH

expression decreased in high glucose-induced rat mesangial cells and streptozotocin-induced diabetic mice [29]. Overexpression of circ-ITCH ameliorates inflammation and fibrosis in the kidneys of diabetic mice [29]. Our study identified downregulated circ-ITCH expression in LPS-stimulated septic mice and HK-2 cells. SCr and BUN are critical indicators of damage to glomerular filtration [30]. Circ-ITCH overexpression reduced serum SCr and BUN levels in LPS-stimulated sepsis mice. Also, circ-ITCH overexpression decreased the levels of AKI-associated markers (NGAL and Kim-1) in LPS-induced sepsis mice. In addition, circ-ITCH elevation alleviated oxidative stress and inflammatory response. These results suggest that circ-ITCH protects renal function in sepsis-induced AKI. Mitochondria are the center of cell energy metabolism and are closely associated with the pathophysiology of sepsis-induced AKI [31]. Mitochondrial dysfunction in AKI is characterized by decreased ATP levels and complexes I/II/III/IV activities [32], which has been observed in

LPS-induced sepsis mice. Circ-ITCH overexpression increased ATP levels and complexes I/II/III/IV activities in LPS-induced sepsis mice. In addition, our observations revealed an upregulation of the mitochondrial fission protein, DRP-1, and a downregulation of mitochondrial fusion proteins, OPA-1 and MFN-1, in LPS-induced sepsis mice. Elevating circ-ITCH expression attenuated DRP-1 levels while enhancing OPA-1 and MFN-1 levels in both LPS-induced sepsis mice and HK-2 cells. Interestingly, another study indicated that expression levels of MFN-2 and DRP-1 remained unchanged in sepsis-AKI patients [33]. To delve deeper into the influence of circ-ITCH on mitochondrial functions, we assessed the OCR, mtDNA copy number, and specific mitochondrial proteins including HSP60 and SDHA. Data indicated that overexpression of circ-ITCH augmented OCR levels and mtDNA copy numbers while diminishing the protein expression levels of HSP60 and SDHA. These findings indicated that circ-ITCH ameliorates mitochondrial dysfunction in sepsis-induced AKI. Furthermore, we found that circ-ITCH mitigated oxidative stress-induced mitochondrial dysfunction by co-treating with NAC (a ROS scavenger) and sh-ITCH in LPS-stimulated HK-2 cells.

Additionally, the molecular mechanism of circ-ITCH protection against sepsis-stimulated AKI was explored, and bioinformatics analysis identified circ-ITCH as a target of miR-214-3p. Inhibition of miR-214-3p promotes proliferation and alleviates oxidative stress and inflammation in LPS-stimulated HK-2 cells. These findings indicated that miR-214-3p plays a critical role in regulating the progression of sepsis-induced AKI. A previous study showed that miR-214-3p suppression inhibited apoptosis and oxidative stress in cisplatin-induced AKI [19]. MiR-214-3p reportedly promotes kidney injury and inflammatory responses in hyperlipidemic pancreatitis [18]. Moreover, miR-214-3p promotes renal inflammatory infiltration in diabetic nephropathy [34]. These data support our results that miR-214-3p acts as a pivotal regulator in the pathogenesis of sepsis-induced AKI. Notably, miR-214-3p inhibition protected mitochondrial function in sepsis-induced AKI, as evidenced by the downregulation of DRP-1 and the upregulation of OPA-1 and MFN-1 expression. MiR-214-3p aggravates chronic kidney disease by disrupting mitochondrial oxidative phosphorylation [35]. The repressive effects of miR-214-3p depletion on sepsis-induced AKI were reversed by circ-ITCH knockdown. Our findings demonstrate that circ-ITCH suppresses oxidative stress and mitochondrial dysfunction in sepsis-induced AKI by regulating miR-214-3p.

Furthermore, the target gene of miR-214-3p was explored, and bioinformatic analysis indicated ABCA1 as a potential target for miR-214-3p. Circ-ITCH promotes ABCA1 expression in sepsis-induced AKI. ABCA1 is a member of a subfamily of ABC transporters, which mainly regulates cellular lipids. Genetic overexpression of ABCA1 has been found to rescue mice with focal segmental glomerulosclerosis [36]. In contrast, ABCA1 deficiency exacerbates renal lipid deposition and kidney injury in diabetic kidney disease [37]. Deficiency of ABCA1 in glomerular endothelial cells led to heightened renal inflammatory damage and increased cellular apoptosis

[37]. In addition, ABCA1 deficiency results in cardiolipin-driven mitochondrial dysfunction in podocytes [38]. Studies have been demonstrated that the increase of ABCA1 decreases proteinuria and renal inflammation [38]. Evidence from this study revealed that ABCA1 expression is downregulated in the renal tissues of mice with LPS-induced sepsis. MiR-214-3p downregulation significantly increased ABCA1 expression in sepsis-induced AKI, which was offset by circ-ITCH knockdown. Additionally, our observations revealed that the knockdown of ABCA1 mitigated the protective effects of circ-ITCH against inflammation and mitochondrial dysfunction in sepsis-induced AKI. These findings suggest that circ-ITCH acts as a buffer for the miR-214-3p/ABCA1 axis, thus diminishing inflammation and mitochondrial impairment in sepsis-induced AKI.

5. Conclusions

Circ-ITCH protects against sepsis-induced AKI by antagonizing inflammation and mitochondrial dysfunction. Circ-ITCH exerts its effects by competitively binding to miR-214-3p and facilitating ABCA1 expression. Our results revealed that circ-ITCH may be a new therapeutic target for sepsis-induced AKI by regulating mitochondrial function. Meanwhile, we proposed an underlying mechanism of circ-ITCH regulation of sepsis-induced AKI by affecting the miR-214-3p/ABCA1 axis. However, the specific mechanism by which the circ-ITCH/miR-214-3p/ABCA1 axis regulates sepsis-induced AKI requires further elucidation. Further *in vitro* and *in vivo* experiments are necessary to determine the role of miR-214-3p/ABCA1 in sepsis-induced AKI.

Acknowledgments

Not applicable.

Author contributions

Weidi Ye: Conceptualization; Data curation, Investigation; Methodology; Visualization; Roles/Writing—original draft. Qi Miao: Conceptualization; Data curation, formal analysis, and visualization. GuangXin Xu: Data curation; Formal analysis. Kai Jin: Data curation, Investigation; Validation. Xue Li: Data curation, Investigation; Funding acquisition, validation. Weidong Wu: Methodology; Supervision; Validation. Lina Yu: Project administration, Resources; Software; Supervision; Validation; Writing, review, and editing. Min Yan: Conceptualization; Project administration, funding acquisition, Supervision; Validation; Writing, review, and editing. All authors have reviewed the results and approved the final version of the manuscript.

Ethical approval

This study was approved by the Institutional Animal Care and Use Committee of The Second Affiliated Hospital of Zhejiang University School of Medicine.

Disclosure statement

No potential conflict of interest was reported by the author(s).

Funding

This research was supported by the (National Natural Science Foundation of China) under Grant [number 82071227]; the (National Clinical Key Specialty Construction Project of China 2021) under Grant [number 2021-LCZDZK-01]; and (Zhejiang Provincial Natural Science Foundation of China) under Grant [number LQ19H090015].

Data availability statement

The datasets used and/or analyzed during the current study are available from the corresponding author upon reasonable request.

References

- [1] Rello J, Valenzuela-Sánchez F, Ruiz-Rodríguez M, et al. Sepsis: a review of advances in management. *Adv Ther*. 2017;34(11):1–17. doi: [10.1007/s12325-017-0622-8](https://doi.org/10.1007/s12325-017-0622-8).
- [2] Peerapornratana S, Manrique-Caballero CL, Gómez H, et al. Acute kidney injury from sepsis: current concepts, epidemiology, pathophysiology, prevention and treatment. *Kidney Int*. 2019;96(5):1083–1099. doi: [10.1016/j.kint.2019.05.026](https://doi.org/10.1016/j.kint.2019.05.026).
- [3] Poston JT, Koyner JL. Sepsis associated acute kidney injury. *BMJ*. 2019;364:k4891. doi: [10.1136/bmj.k4891](https://doi.org/10.1136/bmj.k4891).
- [4] Scholz H, Boivin FJ, Schmidt-Ott KM, et al. Kidney physiology and susceptibility to acute kidney injury: implications for renoprotection. *Nat Rev Nephrol*. 2021;17(5):335–349. doi: [10.1038/s41581-021-00394-7](https://doi.org/10.1038/s41581-021-00394-7).
- [5] Kim SH, Kim H. Inhibitory effect of astaxanthin on oxidative stress-induced mitochondrial dysfunction—a mini-review. *Nutrients*. 2018;10(9):1137. doi: [10.3390/nu10091137](https://doi.org/10.3390/nu10091137).
- [6] Mooli RGR, Mukhi D, Ramakrishnan SK. Oxidative stress and redox signaling in the pathophysiology of liver diseases. *Compr Physiol*. 2022;12(2):3167–3192.
- [7] Mohandes S, Doke T, Hu H, et al. Molecular pathways that drive diabetic kidney disease. *J Clin Invest*. 2023;133(4) doi: [10.1172/JCI165654](https://doi.org/10.1172/JCI165654).
- [8] Doke T, Mukherjee S, Mukhi D, et al. NAD(+) precursor supplementation prevents mtRNA/RIG-I-dependent inflammation during kidney injury. *Nat Metab*. 2023;5(3):414–430. doi: [10.1038/s42255-023-00761-7](https://doi.org/10.1038/s42255-023-00761-7).
- [9] Wu J, Ma Z, Raman A, et al. APOL1 risk variants in individuals of African genetic ancestry drive endothelial cell defects that exacerbate sepsis. *Immunity*. 2021;54(11):2632–2649.e6. doi: [10.1016/j.immuni.2021.10.004](https://doi.org/10.1016/j.immuni.2021.10.004).
- [10] Arulkumaran N, Deutschman CS, Pinsky MR, et al. Mitochondrial function in sepsis. *Shock*. 2016;45(3):271–281. doi: [10.1097/SHK.0000000000000463](https://doi.org/10.1097/SHK.0000000000000463).
- [11] Salzman J. Circular RNA expression: its potential regulation and function. *Trends Genet*. 2016;32(5):309–316. doi: [10.1016/j.tig.2016.03.002](https://doi.org/10.1016/j.tig.2016.03.002).
- [12] Zhong D, Xu GZ, Wu JZ, et al. Circ-ITCH sponges miR-214 to promote the osteogenic differentiation in osteoporosis via upregulating YAP1. *Cell Death Dis*. 2021;12(4):340. doi: [10.1038/s41419-021-03586-y](https://doi.org/10.1038/s41419-021-03586-y).
- [13] Su K, Yi Q, Dai X, et al. Circular RNA ITCH: an emerging multifunctional regulator. *Biomolecules*. 2022;12(3):359. doi: [10.3390/biom12030359](https://doi.org/10.3390/biom12030359).
- [14] Yang C, Yuan W, Yang X, et al. Circular RNA circ-ITCH inhibits bladder cancer progression by sponging miR-17/miR-224 and regulating p21, PTEN expression. *Mol Cancer*. 2018;17(1):19. doi: [10.1186/s12943-018-0771-7](https://doi.org/10.1186/s12943-018-0771-7).
- [15] Han J, Li S, Feng Y, et al. A novel circular RNA (hsa_circ_0059930)-mediated miRNA-mRNA axis in the lipopolysaccharide-induced acute lung injury model of MRC-5 cells. *Bioengineered*. 2021;12(1):1739–1751. doi: [10.1080/21655979.2021.1916276](https://doi.org/10.1080/21655979.2021.1916276).
- [16] Wang ST, Liu LB, Li XM, et al. Circ-ITCH regulates triple-negative breast cancer progression through the wnt/ β -catenin pathway. *Neoplasma*. 2019;66(2):232–239. doi: [10.4149/neo_2018_180710N460](https://doi.org/10.4149/neo_2018_180710N460).
- [17] Liu Y, Usa K, Wang F, et al. MicroRNA-214-3p in the kidney contributes to the development of hypertension. *J Am Soc Nephrol*. 2018;29(10):2518–2528. doi: [10.1681/ASN.2018020117](https://doi.org/10.1681/ASN.2018020117).
- [18] Yan Z, Zang B, Gong X, et al. MiR-214-3p exacerbates kidney damages and inflammation induced by hyperlipidemic pancreatitis complicated with acute renal injury. *Life Sci*. 2020;241:117118. doi: [10.1016/j.lfs.2019.117118](https://doi.org/10.1016/j.lfs.2019.117118).
- [19] Zhou J, Xiao C, Zheng S, et al. MicroRNA-214-3p aggravates ferroptosis by targeting GPX4 in cisplatin-induced acute kidney injury. *Cell Stress Chaperones*. 2022;27(4):325–336. doi: [10.1007/s12192-022-01271-3](https://doi.org/10.1007/s12192-022-01271-3).
- [20] Ferrè S, Deng Y, Huen SC, et al. Renal tubular cell spliced X-box binding protein 1 (Xbp1s) has a unique role in sepsis-induced acute kidney injury and inflammation. *Kidney Int*. 2019;96(6):1359–1373. doi: [10.1016/j.kint.2019.06.023](https://doi.org/10.1016/j.kint.2019.06.023).
- [21] Wang Z, Wu J, Hu Z, et al. Dexmedetomidine alleviates lipopolysaccharide-induced acute kidney injury by inhibiting p75NTR-mediated oxidative stress and apoptosis. *Oxid Med Cell Longev*. 2020;2020:5454210. doi: [10.1155/2020/5454210](https://doi.org/10.1155/2020/5454210).
- [22] Li JH, Liu S, Zhou H, et al. starBase v2.0: decoding miRNA-ceRNA, miRNA-ncRNA and protein-RNA interaction networks from large-scale CLIP-Seq data. *Nucleic Acids Res*. 2014;42:D92–7. doi: [10.1093/nar/gkt1248](https://doi.org/10.1093/nar/gkt1248).
- [23] Peng W, Zhu S, Chen J, et al. Hsa_circRNA_33287 promotes the osteogenic differentiation of maxillary sinus membrane stem cells via miR-214-3p/Runx3. *Biomed Pharmacother*. 2019;109:1709–1717. doi: [10.1016/j.biopha.2018.10.159](https://doi.org/10.1016/j.biopha.2018.10.159).
- [24] Ajay AK, Kim TM, Ramirez-Gonzalez V, et al. A bioinformatics approach identifies signal transducer and activator of transcription-3 and checkpoint kinase 1 as upstream regulators of kidney injury molecule-1 after kidney injury. *J Am Soc Nephrol*. 2014;25(1):105–118. doi: [10.1681/ASN.2013020161](https://doi.org/10.1681/ASN.2013020161).
- [25] Liu X, Wang L, Cai J, et al. N-acetylcysteine alleviates H2O2-induced damage via regulating the redox status of intracellular antioxidants in H9c2 cells. *Int J Mol Med*. 2019;43(1):199–208. doi: [10.3892/ijmm.2018.3962](https://doi.org/10.3892/ijmm.2018.3962).
- [26] Li P, Zhou Y, Goodwin AJ, et al. Fli-1 governs pericyte dysfunction in a murine model of sepsis. *J Infect Dis*. 2018;218(12):1995–2005. doi: [10.1093/infdis/jiy451](https://doi.org/10.1093/infdis/jiy451).

- [27] Zhang D, Han S, Zhou Y, et al. Therapeutic effects of mangiferin on sepsis-associated acute lung and kidney injuries via the downregulation of vascular permeability and protection of inflammatory and oxidative damages. *Eur J Pharm Sci.* 2020;152:105400. doi: [10.1016/j.ejps.2020.105400](https://doi.org/10.1016/j.ejps.2020.105400).
- [28] Brandenburger T, Salgado Somoza A, Devaux Y, et al. Noncoding RNAs in acute kidney injury. *Kidney Int.* 2018;94(5):870–881. doi: [10.1016/j.kint.2018.06.033](https://doi.org/10.1016/j.kint.2018.06.033).
- [29] Liu J, Duan P, Xu C, et al. CircRNA circ-ITCH improves renal inflammation and fibrosis in streptozotocin-induced diabetic mice by regulating the miR-33a-5p/SIRT6 axis. *Inflamm Res.* 2021;70(7):835–846. doi: [10.1007/s00011-021-01485-8](https://doi.org/10.1007/s00011-021-01485-8).
- [30] Stark J. Interpretation of BUN and serum creatinine. An interactive exercise. *Crit Care Nurs Clin North Am.* 1998;10(4):491–496. doi: [10.1016/S0899-5885\(18\)30194-1](https://doi.org/10.1016/S0899-5885(18)30194-1).
- [31] Sun J, Zhang J, Tian J, et al. Mitochondria in sepsis-induced AKI. *J Am Soc Nephrol.* 2019;30(7):1151–1161. doi: [10.1681/ASN.2018111126](https://doi.org/10.1681/ASN.2018111126).
- [32] Li J, Zhang Z, Wang L, et al. Maresin 1 attenuates lipopolysaccharide-induced acute kidney injury via inhibiting NOX4/ROS/NF- κ B pathway. *Front Pharmacol.* 2021;12:782660. doi: [10.3389/fphar.2021.782660](https://doi.org/10.3389/fphar.2021.782660).
- [33] van der Slikke EC, Star BS, van Meurs M, et al. Sepsis is associated with mitochondrial DNA damage and a reduced mitochondrial mass in the kidney of patients with sepsis-AKI. *Crit Care.* 2021;25(1):36. doi: [10.1186/s13054-020-03424-1](https://doi.org/10.1186/s13054-020-03424-1).
- [34] Zhang X, Ren L, Wei J, et al. Silencing long noncoding RNA-CES1P1 suppresses glomerular endothelial cell inflammation in diabetic nephropathy. *Int Immunopharmacol.* 2022;110:108820. doi: [10.1016/j.intimp.2022.108820](https://doi.org/10.1016/j.intimp.2022.108820).
- [35] Bai M, Chen H, Ding D, et al. MicroRNA-214 promotes chronic kidney disease by disrupting mitochondrial oxidative phosphorylation. *Kidney Int.* 2019;95(6):1389–1404. doi: [10.1016/j.kint.2018.12.028](https://doi.org/10.1016/j.kint.2018.12.028).
- [36] Pedigo CE, Ducasa GM, Leclercq F, 3rd, et al. Local TNF causes NFATc1-dependent cholesterol-mediated podocyte injury. *J Clin Invest.* 2016;126(9):3336–3350. doi: [10.1172/JCI85939](https://doi.org/10.1172/JCI85939).
- [37] Zhang J, Wu Y, Zhang J, et al. ABCA1 deficiency-mediated glomerular cholesterol accumulation exacerbates glomerular endothelial injury and dysfunction in diabetic kidney disease. *Metabolism.* 2023;139:155377. doi: [10.1016/j.metabol.2022.155377](https://doi.org/10.1016/j.metabol.2022.155377).
- [38] Ducasa GM, Mitrofanova A, Mallela SK, et al. ATP-binding cassette A1 deficiency causes cardiolipin-driven mitochondrial dysfunction in podocytes. *J Clin Invest.* 2019;129(8):3387–3400. doi: [10.1172/JCI125316](https://doi.org/10.1172/JCI125316).